Coupled Nonlinear Barge Motions, Part I: Deterministic Models Development, Identification and Calibration

Solomon C. S. Yim

Tongchate Nakhata

Ocean Engineering Program,
Oregon State University,
Corvallis, OR 97331

Warren A. Bartel

Erick T. Huang

1100 23rd Avenue,
Naval Facilities Engineering Service Center,
Port Hueneme, CA 93043-4370

This paper focuses on the development of optimal deterministic, nonlinearly coupled barge motion models, identification of their system parameters, and calibration of their prediction capability using experimental results. The ultimate objective is to develop accurate yet sufficiently low degree-of-freedom stochastic models suitable for efficient probabilistic stability and reliability analyses of US Naval barges for preliminary design and operation guideline development (see Part II). First a three-degree-of-freedom (3DOF) fully coupled roll-heave-sway model, which features realistic and practical high-degree polynomial approximations of rigid body motion relations, hydrostatic and hydrodynamic force-moment specifically suitable for barges, is examined. The hydrostatic force-moment relationship includes effects of the barge's sharp edge and combined roll-heave states, and the hydrodynamic terms are in a "Morison" type quadratic form. System parameters of the 3DOF model are identified using physical model test results from several regular wave cases. The predictive capability of the model is then calibrated using results from a random wave test case. Recognizing the negligible sway influence on coupled roll and heave motions and overall barge stability, and in an attempt to reduce anticipated stochastic computational efforts in stability analysis, a two-degree-of-freedom (2DOF) roll-heave model is derived by uncoupling sway from the roll-heave governing equations of motion. Time domain simulations are conducted using the 3DOF roll-heave-sway and the 2DOF roll-heave models for regular and random wave cases to validate the model assumptions and to assess their (numerical) prediction capabilities.
[DOI: 10.1115/1.1854700]

Introduction

In the design of ship-to-shore transport cargo barges, it is essential to determine barge stability for a range of operational and survival sea conditions. In general, the barges will operate in a variety of directional seastates. However, the most unstable scenario is if the barges broach and become broadside to the waves in the so called "beam seas" and may incur large amplitude three-degree-of-freedom (3DOF)—roll, heave, and sway motions with the possibility of capsizing [1]. Many researchers further reduced the DOF of the systems to that of roll only by taking advantage of the dominant roll behavior [2–7]. Parameters for the coefficients of nonlinear roll motions were determined [8] and the roll motions characteristics of full scale ships were examined [9]. A stochastic approach to the analysis of noisy periodic roll motions was proposed [10].

This paper presents a deterministic 3DOF roll-heave-sway model [7,11], and a corresponding two-degree-of-freedom (2DOF) roll-heave model [12,13], to predict barge motion responses. These low DOF models, with high-degree polynomial approximations of force and moment relationships, capable of capturing the important nonlinear characteristics of the coupled nonlinear responses for large roll angle motions, will be used in the development of efficient stochastic models for preliminary design and response predictions under operational and survival conditions (see Part II).

In research conducted earlier at Oregon State University, a one-degree-of-freedom (1DOF) system [10] was developed to model pure roll motion of a barge in random beam seas. Nonlinearities of the model include the righting moment and fluid-structure viscous effects. Hydrodynamic and structural damping effects were approximated by a linear term plus a "Morison" type quadratic term [14]. The righting moment included nonlinear stiffness terms to provide a more accurate restoring moment at larger roll angles. This 1DOF model was compared with measured barge motion data and was found capable of reasonable predictions in terms of statistical moments, spectral densities, and histograms.

In this study, we focus our discussion on a 3DOF deterministic model including the nonlinear coupling effects of roll, heave and sway motions [1,11]. This 3DOF model is expected to improve the predictive capability at large roll angles over the 1DOF system because the heave and sway coupling effects with the roll through hydrostatics and rigid body kinematics are included, and significantly higher degree polynomial approximations are employed. The equations of motion of the rigid barge including hydrostatics are first derived. Waves are then applied and terms modeling the hydrodynamic properties are added. Relative motion effects of the barge with respect to the free surface are included. The effects due to hydrostatics are represented with sufficiently high degree polynomials in the model. Various degree polynomials were examined to identify an optimum fit. Because the edges of the barge are sharp, fairly high degree polynomials are required. The coupling effects of sway on roll-heave response prediction are examined using the roll-heave-sway model and a corresponding 2DOF roll-heave model with similar parameters.

Equations of Motion

Two deterministic mathematical models representative of the physics of the fluid structure interaction for the barge in ocean waves are derived. The motions of a rigid body in air are obtained

Contributed by the OOAE Division for publication in the JOURNAL OF OFFSHORE MECHANICS AND ARCTIC ENGINEERING. Manuscript received August 5, 2003; final revision, March 23, 2004. Review conducted by: R. Riggs.

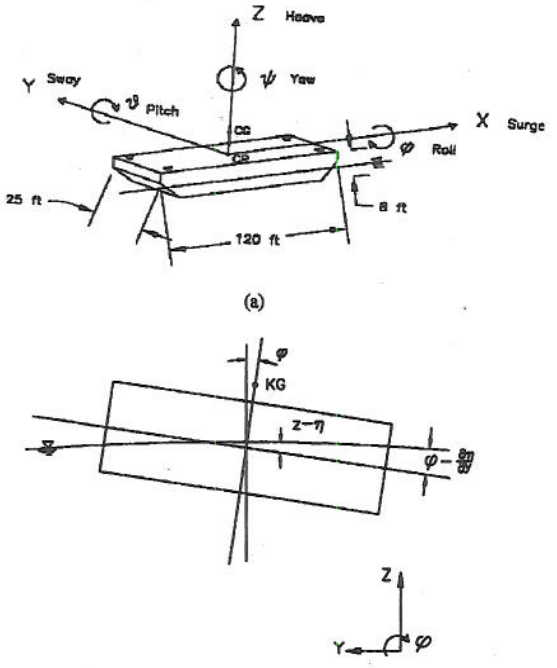

Fig. 1 (*a*) Coordinate system definition and (*b*) relative motion system of barge considered

first and then the barge will be placed in water and the effects due to hydrostatics and hydrodynamics will be included. Once the complete 3DOF model for the barge motions in beam seas is derived, a reduced set of equations of motion (2DOF model) uncoupling sway from roll and heave are derived.

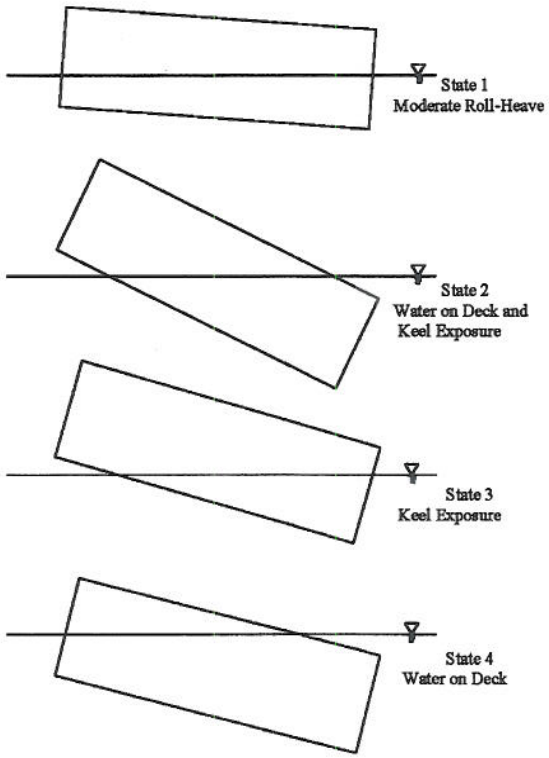

Fig. 2 Four main states of combined roll-heave position of barge motion

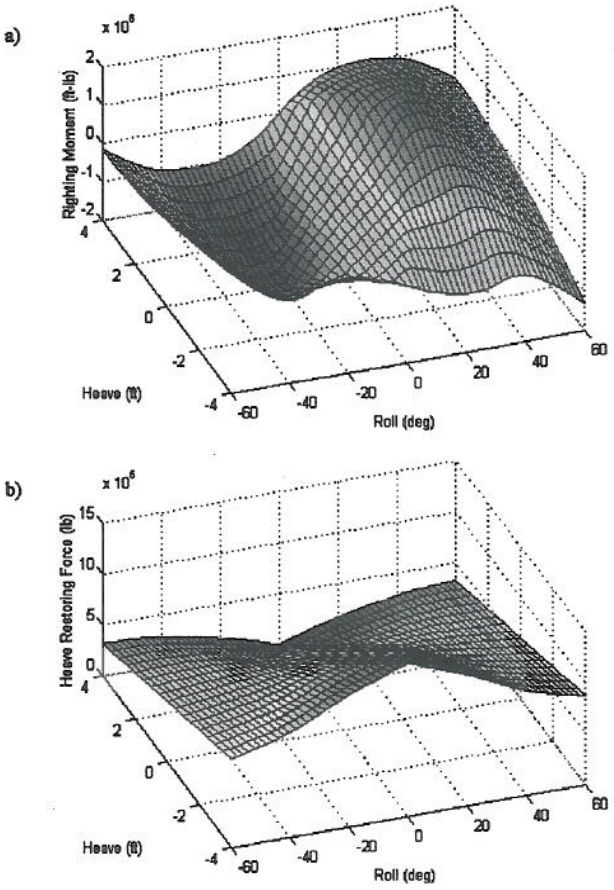

Fig. 3 Analytical surface of (*a*) rol righting moment and (*b*) heave restoring force (*L*=120 ft, *B*=25 ft, *D*=8 ft, draft=4 ft, and KG=9.23 ft)

Model Assumptions. The underlying physical assumptions used in this study for the development of the equations of motion are summarized in this section. The waves are assumed two-dimensional and the wavelengths are significantly longer than the beam (thus the wave profile is linear across the barge). Wave forces and moments are derived about the center of gravity based on static and dynamic equilibrium. The effect of water-on-deck is treated statically, being modeled only in the hydrostatic restoring moment. Along with this assumption is no bulwarks are present. Coefficients of added inertia, added mass and damping are assumed constant. The longitudinal center of gravity is amidships. This is consistent with the physical model in the experimental test data. The barge is symmetric longitudinally and laterally. Radiation and viscous damping are modeled collectively as a linear and a Morison type quadratic term [14]. Barge length, beam, displacement, draft, location of vertical center of gravity (KG), specific weight of water, and roll center are considered variable input parameters. Effects due to a linear mooring stiffness may be switched on or off for sway motions.

The rigid body dynamic equations of motion for the barge are based on Newton's second law that states the rate of change of linear momentum equals the applied forces and the rate of change of angular momentum equals the applied moments [11]:

$$\frac{d}{dt}(mv)=F; \quad \frac{d}{dt}(I\omega)=M \tag{1}$$

An inertial coordinate system is placed at the location of the prescribed body-fixed "roll center" of the barge under static equilibrium. Note the inertial coordinate system coincides with the body-fixed (moving) coordinate system initially. Static roll righting moments and heave buoyant restoring forces are calculated as a function of the position and rotation of the barge about the roll center. Equilibrium of forces and moments are considered about the roll center (the position of which is time dependent with respect to the inertia coordinates) with heave and sway directions respect to the inertial coordinates.

The body-fixed coordinates are defined such that X=surge, Y=sway, Z=heave, ϕ=Roll, Θ=Pitch, and ψ=yaw (Fig. 1). For the (body-fixed) coordinate system origin, the roll center is at the center of gravity of barge and the coordinate system axes are aligned with the principal axes of inertia. One of the main objectives in this study is to extend the equations of motion for a SDOF system in roll to a multi-DOF system. For a symmetric barge in beam seas, the dominant response will be in sway, heave, and roll. The surge, pitch and yaw motions become negligible [11–13]. Equation (1) now becomes

$$F_2=m[\ddot{y}-\dot{\phi}\dot{z}-z_g\ddot{\phi}]$$

$$F_3=m[\ddot{z}+\dot{\phi}\dot{y}-z_g\dot{\phi}^2]$$

$$M_4=I_{44}\ddot{\phi}-m[z_g(\ddot{y}-\dot{\phi}\dot{z})] \tag{2}$$

The coupling terms represent the components of centripetal accelerations on the body arising from the moving (body-fixed) coordinate system and the inertial difference terms represent gyroscopic moments arising from the moving system [11]. We place the origin of the moving coordinate system at an assumed "center of rotation." These equations show the kinematic coupling in the heave and sway equations with extra terms due to the vertical location of the center of gravity not coinciding with the origin of the coordinate system. The longitudinal and lateral centers of gravity coincide with the origin for the barge under study, (i.e., X_g and Y_g are zero) and so those terms do not appear in the equations.

Restoring Forces and Moments. Placing the barge in water will add terms due to the hydrostatic "Archimedes" buoyant restoring forces and moments. As the barge heaves up and down, the available righting energy of the barge in roll changes. Exact expressions relating the effects of heave on the righting moment were derived from analytical geometry. The analytical geometric method for calculation of the righting moment and buoyant heave force begins with the complete arrangement of possible configurations of the barge in water. These cases may be subdivided into combinations of four main states (Fig. 2). As the barge is rotated through the roll angles at a value of heave, the method determines which state the underwater portion falls within and subdivides it into triangular sections. From these triangles, the center of buoyancy may be obtained by averaging all the centroids of each triangle.

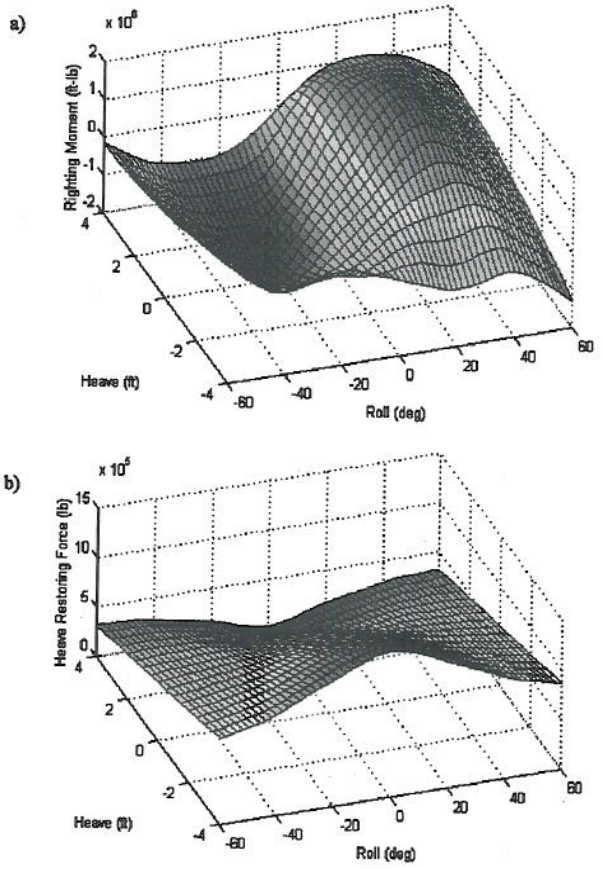

Fig. 4 Polynomial approximation of (*a*) roll righting moment and (*b*) heave restoring force as a function of roll and heave (L=120 ft, B=25 ft, D=8 ft, draft=4 ft, and KG=9.23 ft)

The initial position of the barge is prescribed by a "roll center" with respect to the inertial coordinates. Righting moments are computed over the preset range of roll and heave. This produces a set of righting moment curves for incremental discrete value of heave. The heave range is typically set at maximum value of the barge being totally out of the water at zero roll. The maximum and minimum roll values are determined by sample calculations to see that angle at which the righting moment becomes zero. Analytical expressions of roll righting moment and heave restoring force are graphically shown in Fig. 3.

The matrices of analytical roll restoring moment and heave restoring force are approximated with sufficiently high degree polynomials. Various high and low degree polynomials were tried to determine the optimum fit. The ones which produce errors less than 3% at any combined roll-heave positions are selected. A 13th degree polynomial in roll and 12th degree polynomial in heave were found to be sufficient to qualify the general character of the coupled roll-heave restoring moments. The polynomial fitted roll-righting moment and heave restoring force surfaces are graphically shown in Figs. 4(*a*) and 4(*b*), respectively. The accuracy of the polynomial expressions is determined by examining the differences between the "exact" analytical expressions and the least square fit. The polynomial fit for heave restoring force results in the following expression:

$$R_{33}\left(z,\phi,\eta,\frac{\partial\eta}{\partial y}\right)=[A_{1_1}(z-\eta)^5+A_{1_2}(z-\eta)^4+A_{1_3}(z-\eta)^3+A_{1_4}(z-\eta)^2+A_{1_5}(z-\eta)+A_{1_6}]\left(\phi-\frac{\partial\eta}{\partial y}\right)^{12}+[A_{3_1}(z-\eta)^5$$
$$+A_{3_2}(z-\eta)^4+A_{3_3}(z-\eta)^3+A_{3_4}(z-\eta)^2+A_{3_5}(z-\eta)+A_{3_6}]\left(\phi-\frac{\partial\eta}{\partial y}\right)^{10}+[A_{5_1}(z-\eta)^5+A_{5_2}(z-\eta)^4$$
$$+A_{5_3}(z-\eta)^3+A_{5_4}(z-\eta)^2+A_{5_5}(z-\eta)+A_{5_6}]\left(\phi-\frac{\partial\eta}{\partial y}\right)^{8}+[A_{7_1}(z-\eta)^5+A_{7_2}(z-\eta)^4+A_{7_3}(z-\eta)^3$$
$$+A_{7_4}(z-\eta)^2+A_{7_5}(z-\eta)+A_{7_6}]\left(\phi-\frac{\partial\eta}{\partial y}\right)^{6}+[A_{9_1}(z-\eta)^5+A_{9_2}(z-\eta)^4+A_{9_3}(z-\eta)^3+A_{9_4}(z-\eta)^2$$
$$+A_{9_5}(z-\eta)+A_{9_6}]\left(\phi-\frac{\partial\eta}{\partial y}\right)^{4}+[A_{11_1}(z-\eta)^5+A_{11_2}(z-\eta)^4+A_{11_3}(z-\eta)^3+A_{11_4}(z-\eta)^2+A_{11_5}(z-\eta)+A_{11_6}]$$
$$\times\left(\phi-\frac{\partial\eta}{\partial y}\right)^{2}+[A_{13_1}(z-\eta)^5+A_{13_2}(z-\eta)^4+A_{13_3}(z-\eta)^3+A_{13_4}(z-\eta)^2+A_{13_5}(z-\eta)+A_{13_6}] \tag{3}$$

Similarly, the polynomial expression for the roll restoring moment becomes

$$R_{44}\left(\phi,z,\eta,\frac{\partial\eta}{\partial y}\right)=[B_{1_1}(z-\eta)^4+B_{1_2}(z-\eta)^3+B_{1_3}(z-\eta)^2+B_{1_4}(z-\eta)+B_{1_5}]\left(\phi-\frac{\partial\eta}{\partial y}\right)^{13}+[B_{3_1}(z-\eta)^4+B_{3_2}(z-\eta)^3+B_{3_3}(z-\eta)^2$$
$$+B_{3_4}(z-\eta)+B_{3_5}]\left(\phi-\frac{\partial\eta}{\partial y}\right)^{11}+[B_{5_1}(z-\eta)^4+B_{5_2}(z-\eta)^3+B_{5_3}(z-\eta)^2+B_{5_4}(z-\eta)+B_{5_5}]\left(\phi-\frac{\partial\eta}{\partial y}\right)^{9}$$
$$+[B_{7_1}(z-\eta)^4+B_{7_2}(z-\eta)^3+B_{7_3}(z-\eta)^2+B_{7_4}(z-\eta)+B_{7_5}]\left(\phi-\frac{\partial\eta}{\partial y}\right)^{7}+[B_{9_1}(z-\eta)^4+B_{9_2}(z-\eta)^3$$
$$+B_{9_3}(z-\eta)^2+B_{9_4}(z-\eta)+B_{9_5}]\left(\phi-\frac{\partial\eta}{\partial y}\right)^{5}+[B_{11_1}(z-\eta)^4+B_{11_2}(z-\eta)^3+B_{11_3}(z-\eta)^2+B_{11_4}(z-\eta)+B_{11_5}]$$
$$\times\left(\phi-\frac{\partial\eta}{\partial y}\right)^{3}+[B_{13_1}(z-\eta)^4+B_{13_2}(z-\eta)^3+B_{13_3}(z-\eta)^2+B_{13_4}(z-\eta)+B_{13_5}]\left(\phi-\frac{\partial\eta}{\partial y}\right) \tag{4}$$

These stiffness terms include relative motions between the moving barge and the wave free surface elevation and wave slope changes.

Placing the barge in still water and adding ocean wave excitation introduces terms that represent added mass and added inertia due to relative motion accelerations of the barge and the wave. To take into account energy dissipation effects due to radiation of waves from the barge and flow separation around the hull, the hydrodynamic damping may be modeled as relative motion linear and nonlinear terms. The viscous damping for roll is relative to the time rate of change of wave slope, where the slope is relative to the sway direction (for beam sea conditions).

Roll-Heave-Sway Model. These additional hydrostatic and hydrodynamic force and moment terms are added to the governing equations of motions of the roll-heave-sway model that become

$$m\ddot{y}+m_{a_{22}}\cos\left(\frac{\partial\eta}{\partial y}\right)(\ddot{y}-\dot{v})+m_{a_{33}}\sin\left(\left|\frac{\partial\eta}{\partial y}\right|\right)(\ddot{y}-\dot{v})+C_{22_L}\dot{y}$$
$$+C_{22_N}\dot{y}|\dot{y}|-m\dot{\phi}\dot{z}-m(z_g\cos\phi)\ddot{\phi}$$
$$+R_{33}\left(\phi,z,\eta,\frac{\partial\eta}{\partial y}\right)\sin\left(\frac{\partial\eta}{\partial y}\right)+K_{\text{moor}}y=0$$
$$m\ddot{z}+m_{a_{33}}\cos\left(\frac{\partial\eta}{\partial y}\right)(\ddot{z}-\dot{w})+m_{a_{22}}\sin\left(\left|\frac{\partial\eta}{\partial y}\right|\right)(\ddot{z}-\dot{w})+C_{33_L}\dot{z}$$
$$+C_{33_N}\dot{z}|\dot{z}|+m\dot{\phi}y\dot{y}-m(z_g\cos\phi)\dot{\phi}^2+mg$$
$$+R_{33}\left(\phi,z,\eta,\frac{\partial\eta}{\partial y}\right)\cos\left(\frac{\partial\eta}{\partial y}\right)=0$$
$$I_{44}\ddot{\phi}+I_{a_{44}}\left(\ddot{\phi}-\frac{\partial\ddot{\eta}}{\partial y}\right)+C_{44_L}\left(\dot{\phi}-\frac{\partial\dot{\eta}}{\partial y}\right)+C_{44_N}\left(\dot{\phi}-\frac{\partial\dot{\eta}}{\partial y}\right)\left|\dot{\phi}-\frac{\partial\dot{\eta}}{\partial y}\right|$$
$$+m(z_g\cos\phi)\dot{\phi}\dot{z}-m(z_g\cos\phi)\ddot{y}$$
$$+R_{44}\left(\phi,z,\eta,\frac{\partial\eta}{\partial y}\right)\cos\left(\frac{\partial\eta}{\partial y}\right)-mgz_g\sin\phi=0 \tag{5}$$

Roll-Heave Model. By assuming the influences of sway motion on roll and heave are negligible, the governing equations of motion of the 3DOF roll-heave-sway model, Eq. (5), may be reduced to a 2DOF model in roll and heave only

$$m\ddot{z}+m_{a_{33}}(\ddot{z}-\dot{w})+C_{33_L}\dot{z}+C_{33_N}\dot{z}|\dot{z}|-m(z_g\cos\phi)\phi^2+mg$$
$$+R_{33}\left(z,\phi,\eta,\frac{\partial\eta}{\partial y}\right)=0$$
$$I_{44}\ddot{\phi}+I_{a_{44}}\left(\ddot{\phi}-\frac{\partial\ddot{\eta}}{\partial y}\right)+C_{44_L}\left(\dot{\phi}-\frac{\partial\dot{\eta}}{\partial y}\right)\left|\dot{\phi}-\frac{\partial\dot{\eta}}{\partial y}\right|+C_{44_N}\left(\dot{\phi}-\frac{\partial\dot{\eta}}{\partial y}\right)$$
$$\times\left|\dot{\phi}-\frac{\partial\dot{\eta}}{\partial y}\right|+m(z_g\cos\phi)\dot{\phi}\dot{z}+R_{44}\left(\phi,z,\eta,\frac{\partial\eta}{\partial y}\right)$$
$$-mgz_g\sin\phi=0 \tag{6}$$

Numerical Solution Procedure

To obtain barge motion responses in the time domain based on the roll-heave-sway and the roll-heave models, Eqs. (5) and (6), respectively, are reduced to systems of first order ordinary differ-

ential equations and integrated by standard numerical methods. A fourth order Runge-Kutta method is selected to solve the equations of motion [15].

Regular Waves. A description of the ocean wave field is provided by linear wave theory. The barges considered in this study operate from relatively deep to shallow water. However, the condition of deep water in general produces higher coupling effects of heave on roll due to larger vertical wave velocity. To be conservative in our analysis, therefore, deep-water condition is assumed. For linear regular waves with the assumption of deep water and consideration of water particle kinematics at mean water line, wave expressions are defined as

$$k=\frac{\omega^2}{g}$$

$$\eta=A\sin(ky-\omega t)$$

$$\dot{\eta}=-\omega A\cos(ky-\omega t)$$

$$\ddot{\eta}=-\omega^2\eta$$

$$v=\omega\eta$$

$$\dot{v}=\omega\dot{\eta}$$

$$w=\dot{\eta}$$

$$\dot{w}=-\omega^2\eta$$

$$\frac{\partial\eta}{\partial y}=-\frac{\omega}{g}\dot{\eta}$$

$$\frac{\partial\dot{\eta}}{\partial y}=\frac{\omega^3}{g}\eta$$

$$\frac{\partial\ddot{\eta}}{\partial y}=\frac{\omega^3}{g}\dot{\eta} \tag{7}$$

Measured Random Waves. If measured waves are input to the model, the wave properties as in Eq. (7) are calculated by central difference method. The second and fourth order accurate formulas are, respectively:

$$f'(x_i)=\{f(x_{i+1})-f(x_i)\}/2h$$

$$f''(x_i)=\{f(x_{i+1})-2f(x_i)+f(x_{i-1})\}/h^2$$

$$f'(x_i)=\{-f(x_{i+2})+8f(x_{i+1})-8f(x_{i-1})+f(x_{i-2})\}/12h$$

$$f''(x_i)=\{-f(x_{i+2})+16f(x_{i+1})-30f(x_i)+16f(x_{i-1})-f(x_{i-2})\}/12h^2 \tag{8}$$

Using Eq. (8), the water particle kinematics may be calculated from the measured wave profile.

Simulated Random Waves. For random waves, the wave free surface elevation is represented as a sum of sinusoidal waves with random phases (See. Ref. [14]) by

$$\eta=\sum_{i=1}^{N}\frac{H_i}{2}\sin(k_iy-\omega_it+\varepsilon_i) \tag{9}$$

with parameters determined by the Bretschneider [13] ocean wave spectral model represented by

$$S(\omega)=0.1687\quad H_s^2\frac{\omega_s^4}{\omega^5}e^{-0.675(\omega_s/\omega)^4} \tag{10}$$

Experimental Results

The Naval Facilities Engineering Service Center, Port Hueneme, CA, conducted several measurements of a moored and a partially constrained barge in regular and random seas. Under collaboration with the U.S. Navy, we were provided with a set of measured physical model test data for U.S. Navy model barges, which consists of motions of a 1/16 scale barge in regular and random seas. Free vibration tests of the barge in roll, heave and sway were also conducted to provide estimates of the viscous damping and linear natural periods. The results indicate that 5.25, 4.00, and 27.14 s are the natural periods of roll, heave and sway motion respectively. Table 1 summarizes the parameters of a sample of physical model test cases employed in this study. It should be pointed out here that the barge examined in this study has a vanishing stability of 58 deg (more details, including the GZ curve, are presented in Part II).

Table 1 Physical model test cases

Test case	Wave type	H (ft) or H_s (ft)	T (s) or T_p (s)
SB25	Random	4.7	8.2
SB26	Regular	6.0	5.0
SB27	Regular	6.0	6.0
SB28	Regular	6.0	7.0
SB29	Regular	7.0	8.0
SB30	Regular	6.0	10.0
SB31	Regular	10.0	10.0

Test results from regular wave cases are used to identify system coefficient for both roll-heave-sway and roll-heave models. The tests were conducted with quiescent initial conditions (i.e., zero initial displacements and velocities) and response data were collected after steady-state periodic responses had been achieved. Time domain simulations of varied system coefficients are compared with the test results to determine the best match. The results from random wave case, SB25, are used to calibrate the accuracy of model predictions.

System Parameters Identification

The constant parameters including added mass, added inertia and radiation damping (see Table 2) in the governing equations of motion for roll, sway, and heave are identified using test results of regular waves of heights from 6 to 10 ft and wave periods of 5–10 s (test cases SB26–SB31). Initial approximate values of all system parameters are obtained from a linear potential theory ship motion program developed by Paulling [16–18] based on potential theory. These estimates are then fine-tuned to match the predicted response time series and phase plots with measured results. The resulting identified system parameters are then used as input to the model in the next section to calibrate the accuracy of model prediction for the random wave case (SB25). Because the parameters identified are obtained from the 1/16 scale model test results and not from full-scale prototype tests, these resulting parameters are theoretically suitable for only the scale test model. Higher Reynolds numbers in the full-scale prototype may affect the values of the nonlinear damping coefficient. However, based on numerical model sensitivity studies, the nonlinear damping did not significantly affect the results for the test cases examined in this study. We believe that parameters identified in this section may be extended to the full-scale prototype.

Sample comparison of time histories of the measured versus numerical responses (corresponding to test cases SB27, SB29, and SB30) are shown in Figs. 5–7. It is observed that practically all the parameters estimated by potential theory, are sufficiently accurate for the roll-heave-sway model. Only minor adjustments in the roll added inertia and linear roll damping coefficients are needed to match the measured response well for the all test cases. In addition, for the ranges of wave heights and wave periods considered (SB26–SB31), the identified parameters are practically constant. A summary of the averaged values of the system parameters for regular wave excitations is shown in the second column Table 2. Due to wave drift, the steady-state mean position of the barge motions is down stream of the quiescent, static, equi-

Table 2 Summary of system parameters used in the model

Parameter	Regular wave H from 6 to 10 ft T from 5 to 10 s	Measured random wave H_s=4.7 ft T_p=8.2 s	Simulated random wave H_s=4.7 ft T_p=8.2 s
I_{44} (slugs-ft^2)	2.161E+06	2.161E+06	2.161E+06
I_{a44} (slugs-ft^2)	1.30E+06	1.00E+06	1.00E+06
ζ_{L44}	0.05	0.08	0.03
ζ_{N44}	0.008	0.008	0.008
m (slugs)	2.325E+04	2.325E+04	2.325E+04
m_{a33} (slugs)	1.00E+05	1.00E+05	1.00E+05
ζ_{L33}	0.35	0.35	0.35
ζ_{N33}	0.5	0.5	0.5
m (slugs)	2.325E+04	2.325E+04	2.325E+04
m_{a22} (slugs)	2.00E+04	2.00E+04	1.50E+04
ζ_{L22}	0.5	0.5	0.5
ζ_{N22}	5.0	3.0	3.0

librium position of the moored barge in the experimental setup, where wave elevation was measured. This leads to a time shift (or lag) between the measured wave excitation and barge responses. The wave drift is a function of the wave-height squared and wave period, with larger wave drift magnitude corresponding to larger wave heights. The wave drift also induced tension in the cables used to prevent the barge from drifting down the wave basin. For large wave amplitude excitations (such as SB30, shown in Fig. 7), the almost taut mooring cables induced a small super harmonic component in the roll response.

Figures 5 and 6 show that roll is approximately in-phase with sway and heave is in-phase with wave for all regular wave cases. Case SB27 produces the largest roll motions because the wave period (6 s) is close to the barge roll natural period of 5.25 s, resulting in near resonance.

It is observed that sway is more difficult to match than roll and heave. This is most likely due to the nonlinear mooring cable stiffness, which directly affects the sway motion. A soft mooring in the experiment was required to prevent the model barge from drifting out of the instrumentation area. In this study, the model represents the laboratory sway resistant mooring force by a linear spring. Operationally, in the open sea, the barge would not be moored except possibly under conditions were there might be a cargo transfer from a larger vessel.

Model Prediction Capability Calibration

The roll-heave-sway prediction capability of barge motions under random wave excitations of the 3DOF model is investigated in this section. (A detailed study of the 2DOF model will be presented later.) The averaged identified system parameters of the 3DOF model obtained in the earlier section, with minor adjustments, are used for model predictions for the random wave test case. Measured random waves and simulated random waves are

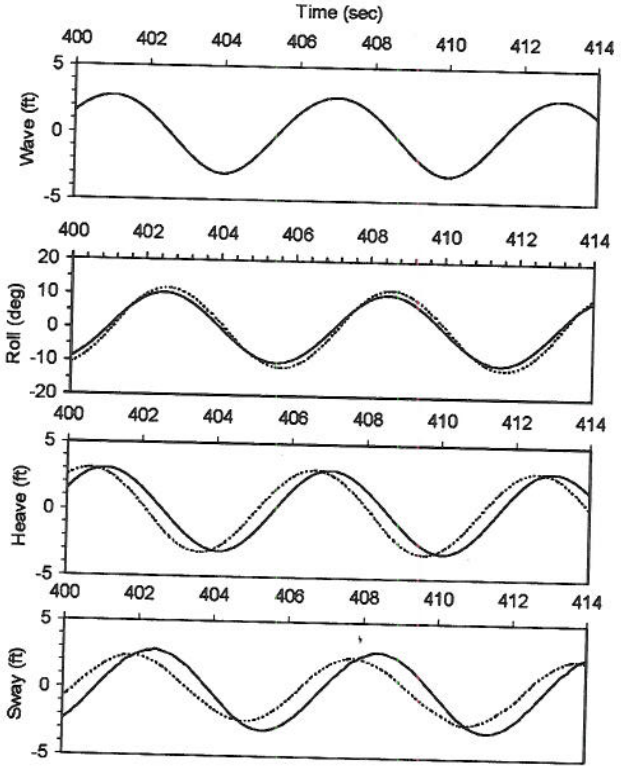

Fig. 5 Barge roll, heave, and sway response time histories to regular waves with H=6 ft and T=6 s (case SB27) (solid line =numerical results, dotted line=experimental results)

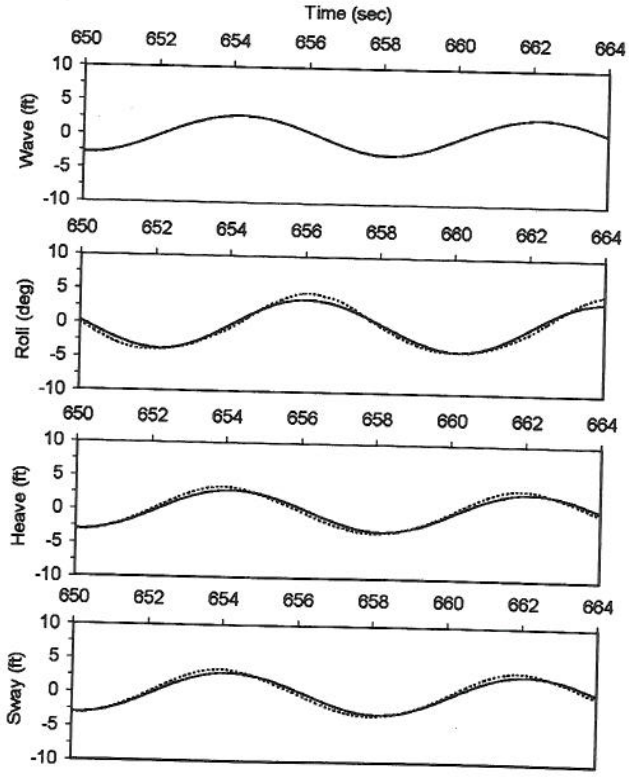

Fig. 6 Barge roll, heave, and sway response time histories to regular waves with H=7 ft and T=8 s (case SB29) (solid line =numerical results, dotted line=experimental results)

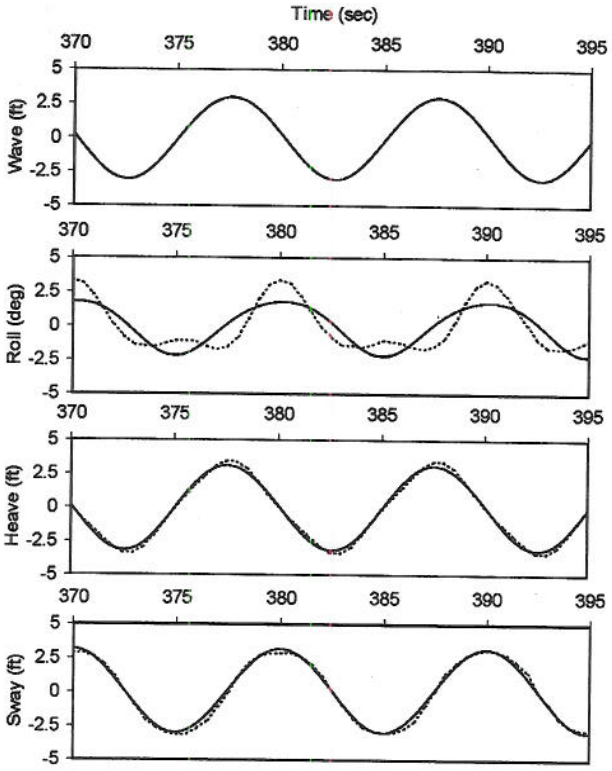

Fig. 7 Barge roll, heave, and sway response time histories to regular waves with H=6 ft and T=10 s (case SB30) (solid line =numerical results, dotted line=experimental results)

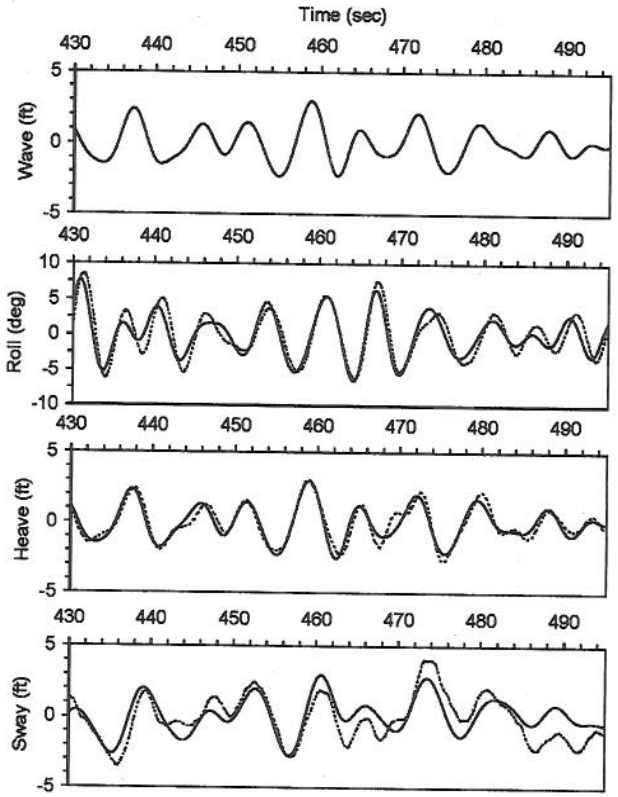

Fig. 8 Comparison of barge motion time histories between 3DOF model predictions and experimental results under random wave excitation with H_s=4.7 ft and T_p=8.2 s (case SB25). Measured waves are used as model input excitation (solid line=numerical results, dotted line=experimental results).

both used as input excitations to the model. Comparisons between model predictions and experimental test results are examined. The accuracy of the model predictions of the barge motions due to random waves is demonstrated using a random wave test case SB25 (H_s=4.7 ft, T_p=8.2 s).

Measured Random Waves. We used the measured random wave profile and numerically derived the wave properties for input to the analytical model. The measured wave was filtered with a low pass tangent Butterworth filter [15] to remove all high frequency wave components above 0.25 Hz (T=4 s) to minimize numerical errors in obtaining derivatives and to adhere to the modeling assumptions that the wavelength is significantly larger than the beam of the barge. We employed the parameters obtained in the earlier section for regular waves. A minor adjustment in the roll linear coefficient from 5% to 8% was found to provide most accurate predictions.

Time histories of the roll-heave-sway model predictions versus measured results are shown in Fig. 8. Observe that the model provides good estimations for both roll and heave motion. It also predicts sway reasonably well. As observed in the regular wave cases, roll is in-phase with sway while heave is in-phase with waves. Note that as indicated in Figs. 6–8, the analytical predictions are in good agreement with the experimental results, well into the highly nonlinear region near the vanishing stability angle of 58 deg. Thus, the analytical models are deemed reliable for prediction of stability behavior of the barge.

The spectral densities of measured results versus the roll-heave-sway model predictions are shown in Fig. 9. Overall, the predictions of spectral densities match the measured results well. The sharp peak around the frequency of 0.03 Hz of the measured sway spectral density probably reflects the nonlinear influence of the mooring cables that is not modeled in this study.

Simulated Random Waves. Gaussian random waves with a significant wave height, H_s=4.7 ft, and spectral peak period, T_p =8.2 s, are simulated by the random wave generation process described in a previous section and used as input into the simulation model. The parameters of the sinusoidal waves are selected to duplicate the statistical and spectral properties of the wave profile specified by the Bretschneider spectrum. As shown in Fig. 10, the spectral densities of the predicted responses matched reasonably well with the experimental results. The model prediction in sway is not as accurate as for roll and heave because of nonlinear characteristics of the mooring cables, which is not modeled in this study.

Sway on Roll and Heave Motions Coupling Effects

The coupling effects of sway on barge roll and heave motions is examined in this section by comparing numerical results of the 3DOF and the 2DOF models using the same analytical procedure conducted in the earlier sections. Identical system parameters are employed in both models (when applicable). Responses to regular and random waves are examined. Figure 11 shows the time histories of barge responses to regular waves with H=6 ft and T =6 s (case SB27) while Fig. 12 shows the time histories of barge responses to measured random waves with H_s=4.7 ft and T_p =8.2 s, respectively. Figure 13 shows the spectral densities of barge responses based on the 3DOF and the 2DOF models subjected to simulated random waves. Observe that both models provide comparable predictions for both regular and random waves. However, the 2DOF model appears to produce slightly larger roll amplitude than those of the 3DOF model.

A preliminary sensitivity study on barge response to regular wave excitation is conducted using both 3DOF and 2DOF models. Barge responses due to several regular waves with various wave heights and wave period are examined. Figure 14 shows amplitudes of periodic roll responses for the barge subjected to regular waves with fixed wave height of 6 and 10 ft, varying the wave

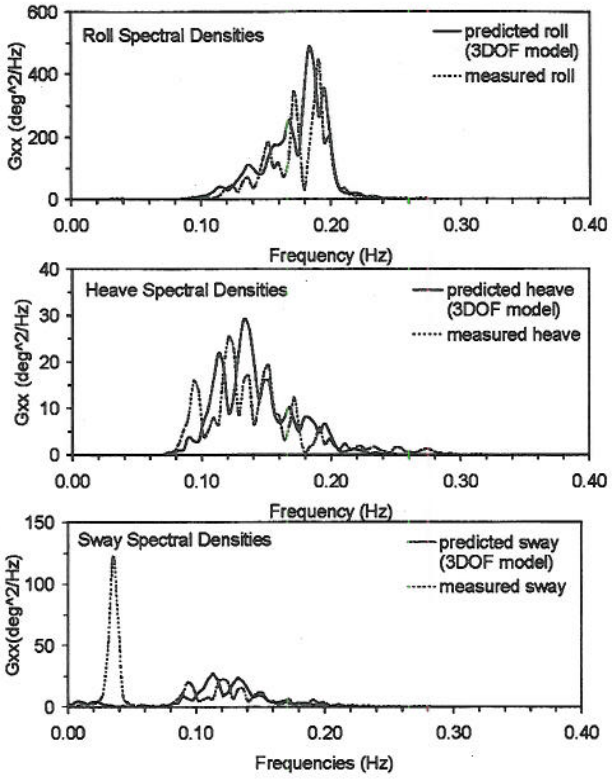

Fig. 9 Comparison of barge motion response spectral densities between 3DOF model predictions and experimental results under random wave excitation with H_s=4.7 ft and T_p=8.2 s (case SB25). Measured waves are usedas model input excitation.

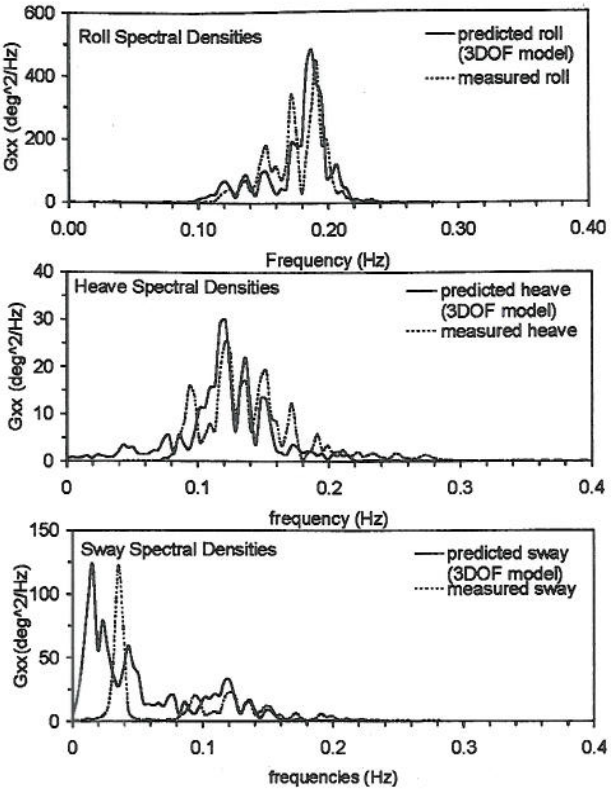

Fig. 10 Comparison of barge motion spectral densities between 3DOF model predictions and experimental results under random wave excitation with H_s=4.7 ft and T_p=8.2 s (case SB25). Simulated random waves are used as model input excitation.

period between 6 and 9 s. Roll amplitude decreases with increasing wave period because the natural frequency for roll motion is 5.25 s. The 3DOF model usually produces slightly lower roll response amplitude than the 2DOF model. Figure 15 shows the roll amplitude response as a function of wave height for the 3DOF and 2DOF systems. It can be observed that predictions from both models matches well over the range of wave heights considered. These results indicate that the effects of moored sway on roll motion could be considered as additional energy dissipation (damping). It is observed that, for moored barges, sway does not produce noticeable effect on heave motion. However, under operations conditions in the open sea, with no mooring, this effect may not be negligible. For an unmoored barge, the wave-induced drift can cause significant sway, and the wave profile and kinematics should be evaluated at the instantaneous position of the barge. This may introduce important nonlinear coupling among the three motions.

Concluding Remarks

The equations of motion for roll, heave, and sway of a barge in random beam seas have been derived. The model was developed based on rigid body dynamics, coupled with relative motion hydrostatic and hydrodynamic terms. The analytical expressions of the relative motion hydrostatic terms are derived based on the four main states for combined roll-heave positions. The relative motion hydrodynamic terms are in a Morison type quadratic form. The relative motion hydrostatic terms, roll righting moment and heave restoring force, are fitted with sufficiently high degree polynomials. A 13th degree polynomial in roll and a 12th degree polynomial in heave are sufficient to qualify the general character of the coupled roll-heave restoring moments.

System parameters for the model are identified by matching numerical predictions in the time domain with experimental results of six regular wave test cases, with initial approximate values of the system parameters obtained based on the potential theory. Only minor adjustments to these estimates are needed to obtain optimal match with experimental results. The same set of system parameters is applicable for all the regular-wave cases considered, which ranges in wave period from 6 to 10 s.

With the identified system parameters from the regular wave cases, it is found that the 3DOF model provides accurate predictions of barge responses to random waves. Two distinctive processes are used to generate random waves for the models. In the first case, the exact measured random wave data is used as input to the numerical models with other wave properties derived numerically. In the second case, a sum of sinusoidal waves with random phases is used to simulate the wave profiles and associated properties. Results from both cases were compared with experimental data. All comparisons indicate close agreement with the model predictions.

The coupling effects of sway on roll and heave barge motions are examined by comparing numerical results from the 3DOF and the 2DOF models employing identical system parameters. Results indicate that the two models provide comparable roll and heave predictions for both regular and random wave cases. It is observed that, for moored barges, the coupling effects of sway on barge roll and heave motions are negligible for the range of system and excitation parameters considered.

The authors believe that these predictive models should be continually improved and kept easy to use as a practical tool for the barge designer and (later barge operators) to quickly assess optimum conditions for designing barge shapes and understanding

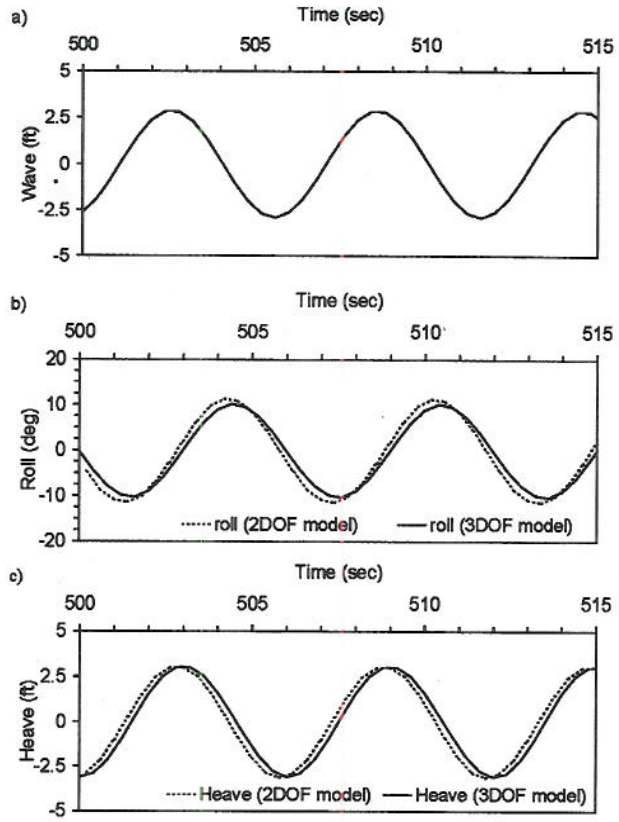

Fig. 11 Comparison of 3DOF and 2DOF model predictions of time histories of roll and heave barge responses under regular wave excitation with H=6 ft and T=6 s (case SB27)

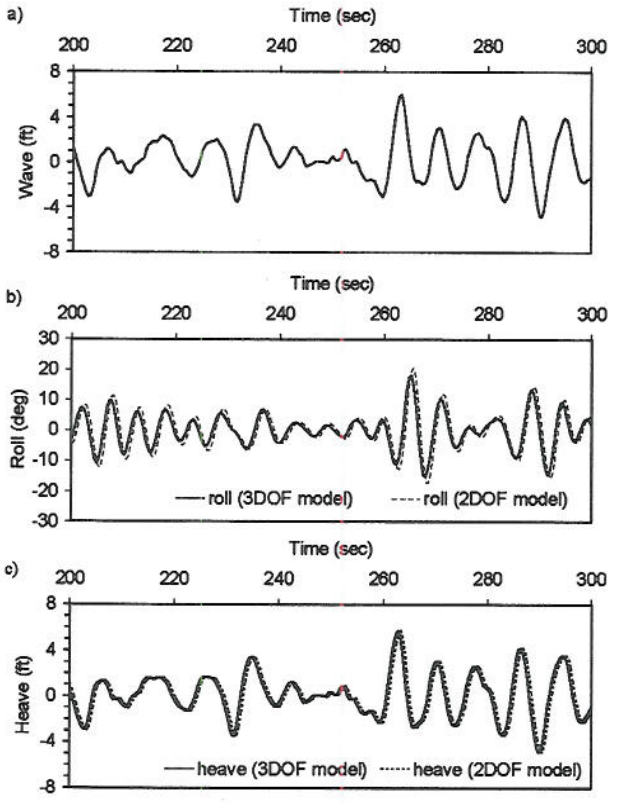

Fig. 12 Comparison of 3DOF and 2DOF model predictions of time histories ofroll and heave barge response under measured random waves with H_s=4.7 ft and T_p=8.2 s (case SB25)

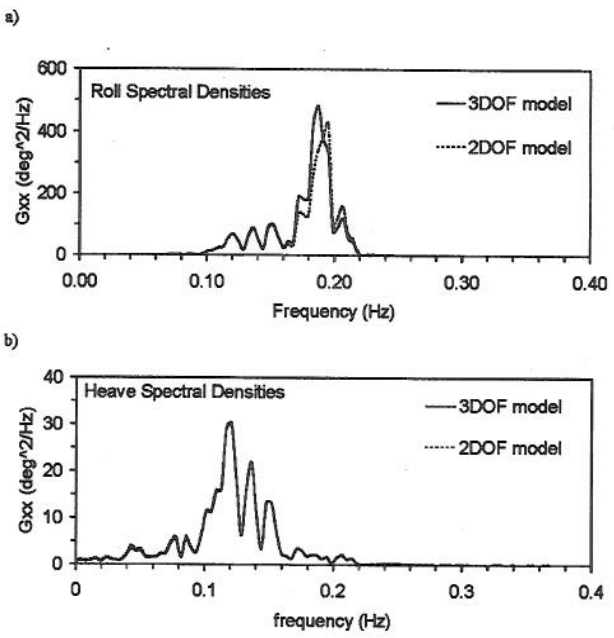

Fig. 13 Comparison of 3DOF and 2DOF model predictions of (*a*) roll and (*b*) heave spectral densities of barge responses under simulated random waves with H_s=4.7 ft and T_p=8.2 s (case SB25)

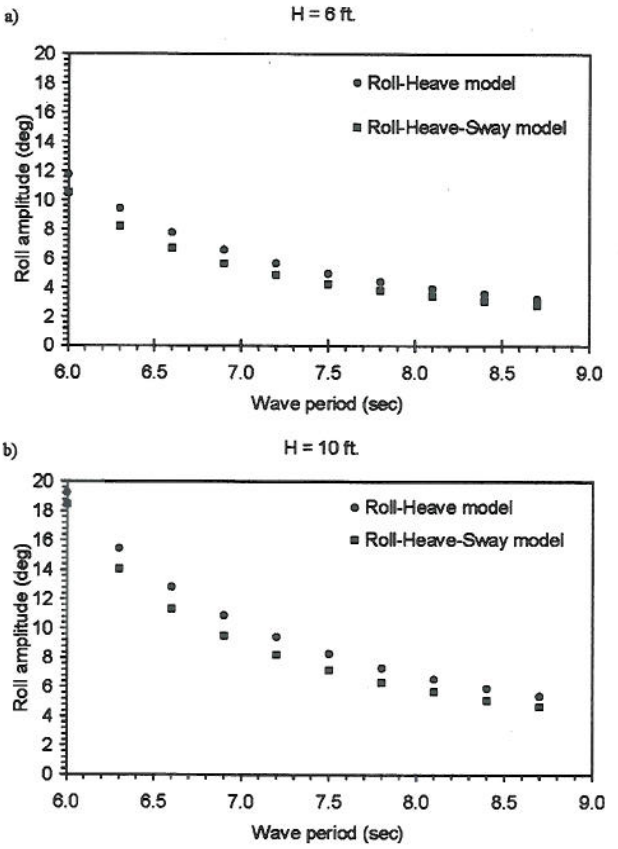

Fig. 14 Predicted periodic roll response amplitude as a function of regular wave period, with wave height (*a*) H=6 ft and (*b*) H=10 ft

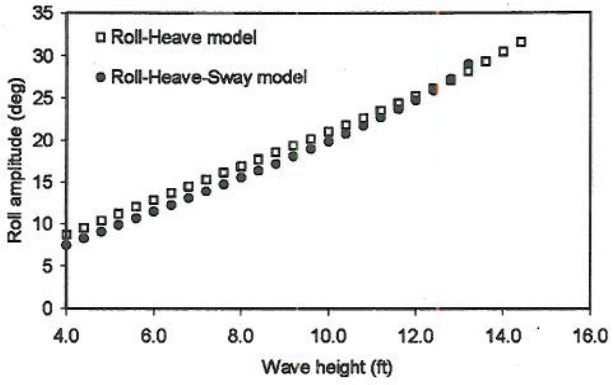

Fig. 15 Predicted periodic roll response amplitude as a function of regular wave height using 3DOF and 2DOF models under fixed wave period $T=6$ s

cargo limitations to mitigate the risk of capsize in beam seas. The models were developed with low dynamic degrees-of-freedom in mind for future efficient (especially stochastic) computational execution while also trying to capture the most important physical parameters for a barge in beam seas.

Acknowledgments

The authors wish to thank the reviewers for their valuable comments and suggestions. Financial support from the United State Office of Naval Research Grant No. N00014-92-1221 is gratefully acknowledged. The authors also wish to acknowledge the Office of Naval Research Seabased Logistics Program under, Dr. P. Abraham, code 362, for support of investigation of the assessment of barge stability.

References

[1] Chen, S.-L., Shaw, S. W., and Troesch, A. W., 1999, "A Systematic Approach to Modelling Nonlinear Multi-DOF Ship Motions in Regular Seas," J. Ship Res., **43**(1), pp. 25–37.

[2] Virgin, L. N., and Bishop, S. R., 1988. "Catchment Regions of Multiple Dynamic Responses in Nonlinear Problems of Offshore Mechanics," Proceedings at 7th International Conference on Offshore Mechanics and Arctic Engineering, Houston, TX, pp. 15–22.

[3] Falzarano, J. M., Shaw, S. W., and Troesch, A. W., 1992, "Application of Global Methods for Analyzing Dynamical Systems to Ship Rolling Motion and Capsizing," Int. J. Bifurcation Chaos Appl. Sci. Eng., **2**(1), 101–116.

[4] Virgin, L. N., and Erickson, B. K., 1994, "A New Approach to the Overturning Stability of Floating Structures," Ocean Eng., **21**(1), pp. 67–80.

[5] Martin, J. P., 1994, "Roll Stabilization of Small Ships," Mar. Technol., Soc. J., **31**(4), pp. 286–295.

[6] Falzarano, J., and Taz Ul Mulk, M., 1994, "Large Amplitude Rolling Motion of an Ocean Survey Vessel," Mar. Technol., Soc. J., **31**(4), pp. 278–285.

[7] Thompson, J. M. T., 1997, "Designing Against Capsize in Beam Seas: Recent Advances and New Insights," Appl. Mech. Rev., **50**(5), pp. 307–325.

[8] Zhang, Y. Z., and Haddara, M. R., 1993, "Parametric Identification of Nonlinear Roll Motion Using Roll Response," International Shipbuilding Progress, **40**, pp. 299–310.

[9] Haddara, M. R., and Wishahy, M., 2002, "An Investigation of Roll Characteristics of Two full Scale Ships at Sea," Ocean Eng., **29**, pp. 651–666.

[10] Lin, H., and Yim, S. C. S., 1995, "Chaotic Roll Motion and Capsizing of Ships Under Periodic Excitation with Random Noise," Appl. Ocean. Res., **17**(3), pp. 185–204.

[11] Abkowitz, M. A., 1969, *Stability and Motion Control of Ocean Vehicles*, MIT Press, Cambridge, MA.

[12] Falzarano, J., and Papoulias, F. (editors), 1993, "Nonlinear Dynamics of Marine Vehicles: Modeling and Applications, Bound Volume to Sessions," ASME Winter Annual Meeting, OMAE/DSC pp. 125.

[13] Liaw, C. Y., Bishop, S. R., and Thompson, J. M. T., 1993, "Heave-Excited Rolling Motion of a Rectangular Vessel in Head Seas," Int. J. Offshore Polar Eng., **3**(1), pp. 26–31.

[14] Chakrabarti, S. K., 1994, *Hydrodynamics of Offshore Structures*, Computational Mechanics Publications, Southampton.

[15] Press, W. H., Flannery, B. P, Teukolsky, S. A., and Vetterling, W. T., 1986, *Numerical Recipes*, Cambridge University Press, Cambridge.

[16] Paulling, J. R. 1990, "Inclusion of Theoretical Achievements in the Field of Stability in the Ship Design Process," STAB '90, Fourth International Conference on Stability of Ships and Ocean Vehicles, Naples, Italy.

[17] Paulling, J. R., 1961, "The Transverse Stability of a Ship in a Longitudinal Seaway," J. Ship Res., **5**(1), pp. 37–49.

[18] Paulling, J. R., and Rosenberg, R. M., 1959, "On Unstable Ship Motions Resulting From Nonlinear Coupling," J. Ship Res., **3**, p. 36.